Embedded-atom calculations of Auger and x-ray photoemission shifts for metallic elements

R. M. Nieminen

Department of Physics, University of Jyväskylä, 40720 Jyväskylä, Finland

M. J. Puska

Laboratory of Physics, Helsinki University of Technology, 02150 Espoo 15, Finland
(Received 18 May 1981)

Change in self-consistent-field energy density-functional calculations are reported for Auger and core-level binding-energy shifts in *sp*-bonded metals. The basic model, atom in jellium vacancy, gives good agreement with experiment, especially in the Auger case. The chemical and relaxation contributions to the shifts are discussed, and the extra-atomic response is analyzed in detail, both in position and energy space. The adequacy of the "excited-atom" approach to the energy shifts is discussed.

I. INTRODUCTION

The kinetic-energy shifts of electrons ejected in core-level photoemission (XPS) and Auger processes between free atoms and condensed phases have been the subject of considerable experimental study.[1] These shifts, while useful in analytic applications of electron spectroscopy, are interesting in their own right; they characterize the effect on the electron-emitting atom of its electronic environment, and thus provide information about the chemical bonding properties of atoms. Of special interest are metallic elements, where the shifts can be substantial. Advances in electron spectroscopy have produced a wealth of data on photoshifts in metallic binding situations. Recent experimental efforts have also made available accurate results for Auger energy shifts between vapor and condensed metallic phases for a number of elements.[2,3]

It was realized early on that the kinetic energy shifts reflect the effects of environment via two contributions: (i) the chemical shift in the initial state of the atom in the condensed situation and (ii) the relaxation shift due to the extra-atomic screening of the hole(s) produced in the final state. However, detailed *ab initio* theoretical studies of the origin and systematics of the shifts are quite scarce. This is understandable as the presence of core hole(s) in the ionized atom breaks the symmetry of the system and makes an *ab initio* calculation difficult, comparable to an impurity problem. Simplified models for the screening charge have been proposed with variable degree of success. Recently, a semiempirical[4] scheme to obtain the metallic photoshifts has been proposed; it is based on bulk cohesive energies, heats of solution, and atomic ionization energies. The relatively good success of this thermochemical model also for

dilute alloys[5] and for Auger processes[2,3] suggests that its ultimate microscopic explanation would be related to those of the Miedema rules[6] for alloying. Another line of models is based on the "excitonic"[7] or "excited-atom"[8] approach, where the basic idea is to assign the extra-atomic screening charge to the first unoccupied valence orbitals of the free ion. While such models have provided much insight into deep-level spectroscopy, especially in the case of transition metals,[9] they are not universally applicable and fail to give good answers or correct trends in cases where the true metallic screening charge is bound to reside outside the outermost valence shell.

In this paper we present results of *ab initio* calculations of x-ray photoemission and Auger energy shifts between free atoms and condensed phases for a number of nontransition metals. The calculations are of (ΔSCF) change in energy of the self-consistent-field type[10] and we employ the self-consistent spin-density-functional[11] method; total energy calculations are carried out for each required configuration. For atoms in metals, a model is used which emphasizes the extended nature of the conduction electrons. The model is closely related to those used by Almbladh and von Barth[12] and Bryant and Mahan[13] for x-ray absorption, and by Lang and Williams[14] for core holes in chemisorbed atoms. Strikingly good agreement with experiment is found, especially in the Auger case, where the shifts are large and have recently[2,3] been accurately obtained in high-temperature vapor-solid experiments. The various contributions to shifts are discussed, both in position and energy space. The results corroborate the idea of the metallic environment of providing a rather structureless source of screening electrons.

The remainder of the paper is organized as follows. In Sec. II we outline the calculational methods. Sec-

tion III contains the results, their analysis and comparison with experiment. Section IV contains a short summary and conclusions.

II. METHOD OF CALCULATION

The focus of our attention is the difference between kinetic energies of electrons emitted from free atoms and atoms in metal. It is thus essential to use as identical analytic approaches as is possible in both cases. We perform in each case two calculations of the electron (spin) densities and the total energy; one for the initial and one for the final state. Thus the shift involves four independent total-energy calculations, and the energy differences can be associated with changes in the kinetic energies of the ejected electrons. This ΔSCF approach assumes a fully developed screening of the core holes (adiabatic limit), and leaves all questions related to dynamic aspects (line shapes, shakeup, etc.) beyond the scope of the present paper. We merely predict the positions of the leading edges of the main photo- or Auger electron lines.

We are dealing here with many-electron states and consequently questions about proper treatment of exchange and correlation arise. The density-functional theory we shall use is formally justified for the lowest energy state of a specified angular and spin symmetry.[15] However, there is no formal justification for using the customary local-density approximation for exchange and correlation for (excited) states constrained to have one or more core holes. Nevertheless there is ample empirical evidence for the accuracy of local-density theory in calculations of, say, ionization potentials[16] or core-level binding energies.[12] Our primary concern here are the extra-atomic effects associated with metallic charge transfer and screening; while the local-density approximation does affect the position of any given spectral line, the difference between the energies corresponding to free atoms and atoms in metal is much less sensitive to it.

The free-atom and ion calculations were carried out using a nonrelativistic, spin-polarized program. The spin densities and the total energy were obtained by solving the equations (in atomic units $\hbar = m = e = 1$)

$$(-\tfrac{1}{2}\nabla^2 + V^s_{\text{eff}}[n^+, n^-, \vec{r}])\psi^s_i(\vec{r}) = \epsilon^s_i \psi_i(\vec{r}) \ , \quad (1)$$

$$n^s(\vec{r}) = \sum_i |\psi^s_i(\vec{r})|^2 ; \quad s = +, - \ , \quad (2)$$

self-consistently. V_{eff} consist of the external potential, Hartree electrostatic, and exchange-correlation contribution. The Gunnarsson-Lundqvist[15] formulas for exchange and correlation were used in the local-density approximation.

For the case of atoms in metal, the atom-in-

jellium-vacancy model[13,17] was adopted as the basic one; refinements to this (in particular, the spherical solid model[12]) were employed, but they turned out to be unnecessary in the sense that they resulted in only minor changes in the shift values (see below).

In the atom-in-jellium-vacancy model the metallic environment of the electron-emitting atom is mimicked by a uniform background of charge with a spherical cavity in it. The volume of this cavity is equal to the Wigner-Seitz cell volume in the condensed phase. The density n_0 of the positive background charge is determined by the metal valency Z_h and the Wigner-Seitz sphere radius R_{WS}, and is conventionally expressed in terms of a density parameter r_s via $n_0 = 3/4\pi r_s^3 = 3Z_h/4\pi R_{\text{WS}}^3$. This is the only parameter in the basic model. The nucleus (charge Z) of the atom in focus is placed in the center of the vacancy, and the spin-density-functional equations (1) and (2) are solved for the combined system. Now in addition to bound (core) states localized at the atom, a band of delocalized (scattering) states exists and the latter are occupied up to the metal Fermi energy. These states are of course responsible for screening and contribute most of the extra-atomic shifts. The details of the calculational procedures have recently been discussed in the context of atoms in electron gas[18]; basically similar routines were used in the present work.

In the spherical solid model[12] features of the discrete lattice potential surrounding the central atom are introduced by including the spherical average of the ion potentials instead of the jellium-vacancy potential. If the host ions are represented by pseudopotentials this is a relatively easy task, and the main effects of lattice discreteness and finite ion core size can be incorporated.

In the calculations of the excited-state energies the appropriate spin-orbital configurations were chosen to be the same for both free atoms and atoms in metal. All charge and spin densities were taken to be spherically symmetric, which amounts to solving the radial equations self-consistently for the relevant spin-orbital occupation numbers. For each element six basic calculations were carried out: (i) free-ground-state atom, (ii) ground-state atom-in-metal, (iii) free-atom with one (inner-shell) core hole, (iv) atom-in-metal with one (inner-shell) core hole, (v) free-atom with two (outer-shell) core holes, and (vi) atom-in-metal with two (outer-shell) core holes. In the cases with two core holes, we generally take them to be in relative spin-triplet state.

The kinetic energies of the photoemitted and Auger electrons are obtained from total-energy differences. In an experimental evaluation of the shifts a common reference level must be agreed upon. In the atomic case a natural reference level is the vacuum, whereas for the (grounded) metal sample the Fermi level, below the vacuum level by the

work function ϕ,[19] is the convenient one. The Fermi level is the reference level also in the metallic calculations, since the necessary perfect screening implies the addition of one electron per core hole on the Fermi level. The free-atom-metal shifts for XPS and Auger cases are then (both referenced to the vacuum level)

$$\Delta_{XPS} = (E_{(iii)} - E_{(i)}) - (E_{(iv)} - E_{(ii)}) - \phi \ , \qquad (3)$$

$$\Delta_{Auger} = (E_{(iv)} - E_{(vi)}) - (E_{(iii)} - E_{(v)}) - \phi \ . \qquad (4)$$

Above, E denotes total energy and the subscripts refer to the configurations (i)–(vi) explained above. Δ_{XPS} is by definition the apparent decrease in core-level binding energy in going to the condensed situation, while Δ_{Auger} is the extra kinetic energy obtained in a solid-state or molecular environment.

III. RESULTS

The elements studied, the investigated core-hole configurations, the density parameters r_s and the free-electron Fermi energies ϵ_F, and the experimental solid-phase work functions are given in Table I. The choice of the elements was influenced by the availability of accurate Auger data.[2,3] Transition metals were avoided since it was felt that the basic model is less adequate for them; this point is further discussed in Sec. IV.

Table II lists the values of the core-level binding and Auger energies. We estimate the numerical errors in the binding and Auger energies and their free-atom-metal shifts to be less than 0.1 eV for Mg and Al and less than 0.5 eV for Zn and elements Ag through Te. This numerical error is mainly caused by subtracting total energies, which are nearly equal, large numbers. Experimental values (see also exten-

sive tabulations of Refs. 3 and 4) are also included. For single ionization, we find that the ΔSCF calculated absolute values for the binding energy of the $1s$ electron for Mg and Al are lower by $\sim$10 eV than the experimental values. This reflects the general feature of the inadequacy of the local-density approximation for very deep, localized core levels. Nonlocal corrections would amount to reducing the Coulombic self-interaction errors inherent in the local-density approximation and would thus increase the binding for the $1s$ levels. For the $2p$ level in Zn we likewise find a slightly too low absolute binding energy compared to the experimental one for $2p_{3/2}$. From calculations with single $3d$ holes for elements Ag through Te we learn that the binding energies agree rather well with the relativistic Hartree-Fock-Slater calculations of Huang et al.[25] for $3d_{3/2}$ electrons. Taking into account the average $3d_{3/2} - 3d_{5/2}$ splitting of $\sim$6 eV for these elements, the agreement with experiment is also quite good. For the $4d$ shell, agreement with the experimental $4d_{3/2}$ values is rather good, too. Our values for the $4d_{3/2}$ binding energy for these fifth-row elements are larger by about 2.5 eV than those calculated by Huang et al.[25]

The absolute values of the atomic Auger energies are also given in Table II together with their experimental values. For the KLL transitions in Mg and Al, the discrepancy with the mean value of $KL_{2,3}L_{2,3}$ energies for the ^1D and ^1S final-state assignments is less than 3 eV. In the case of the LMM line in Zn, the calculated value is somewhat smaller than the L_2,L_3 group average of the $^3P,^3F$ final-state assignments, which is the experimental counterpart that suggests itself for comparison with the calculation for two $3d$ holes in relative spin-triplet state. The MNN Auger energies calculated for atoms Ag through Te are close to the configurational averages over the M_4,M_5 groups of experimental Auger lines with the $^3P,^3F$ final-state assignments.

TABLE I. Basic data for the calculations. The values of the work function ϕ are polycrystalline averages from Ref. 19.

Element	Hole states investigated	r_s	ϵ_F (eV)	ϕ (eV)	Metal valency Z_h
$_{12}$Mg	$1s\downarrow, 2p\downarrow, 2p\downarrow\downarrow$	2.65	7.1	3.7	2
$_{13}$Al	$1s\downarrow, 2p\downarrow, 2p\downarrow\downarrow$	2.07	11.7	4.2	3
$_{30}$Zn	$3p\downarrow, 3d\downarrow, 3d\downarrow\downarrow$	2.31	9.4	3.6	2
$_{47}$Ag	$3d\downarrow, 4d\downarrow, 4d\downarrow\downarrow$	3.02	5.5	4.6	1
$_{48}$Cd	$3d\downarrow, 4d\downarrow, 4d\downarrow\downarrow$	2.59	7.5	4.1	2
$_{49}$In	$3d\downarrow, 4d\downarrow, 4d\downarrow\downarrow$	2.41	8.6	4.1	3
$_{50}$Sn	$3d\downarrow, 4d\downarrow, 4d\downarrow\downarrow$	2.22	10.2	4.4	4
$_{51}$Sb	$3d\downarrow, 4d\downarrow, 4d\downarrow\downarrow$	2.14	10.9	4.7	5
$_{52}$Te	$3d\downarrow, 4d\downarrow, 4d\downarrow\downarrow$	2.08	11.5	4.9	6

TABLE II. Core-level binding and Auger energies for free atoms.

Element and hole configuration		Core-level binding or Auger energy (eV)		Comments
		This work	Experimental or semiexperimental	
Mg	$1s\downarrow$	1300.8	1311.2	Ref. 20
	$2p\downarrow$	58.3	57.6	$3p_{3/2}$; semiempirical; Ref. 4
	$1s\downarrow \rightarrow 2p\downarrow\downarrow$	1159.1	1161.6	^1S; Ref. 21
Al	$1s\downarrow$	1556.1	1568.8	Interpolation Ne-Ar; Ref. 3
	$2p\downarrow$	82.4	81.8	$2p_{3/2}$; semiempirical; Ref. 4
	$1s\downarrow \rightarrow 2p\downarrow\downarrow$	1364.0		
Zn	$2p\downarrow$	1027.0	1029.1	$2p_{3/2}$; Ref. 20
	$3d\downarrow$	18.8	17.3	$3d_{5/2}$; semiempirical; Ref. 4
	$2p\downarrow \rightarrow 3d\downarrow\downarrow$	972.0	975	average; Ref. 21
Ag	$3d\downarrow$	381.2	375.6	$3d_{5/2}$; Ref. 22
	$4d\downarrow$	13.9	12.6	$4d_{5/2}$; semiempirical; Ref. 4
	$3d\downarrow \rightarrow 4d\downarrow\downarrow$	341.0	339	average; Ref. 22
Cd	$3d\downarrow$	418.5	412.3	$3d_{5/2}$; Ref. 22
	$4d\downarrow$	19.3	17.7	$4d_{5/2}$; semiempirical; Ref. 4
	$3d\downarrow \rightarrow 4d\downarrow\downarrow$	366.3	365	average; Ref. 23
In	$3d\downarrow$	459.3	451.7	$3d_{5/2}$; interpolation Cd-Xe; Ref. 4
	$4d\downarrow$	26.9	24.6	$4d_{5/2}$; semiempirical; Ref. 4
	$3d\downarrow \rightarrow 4d\downarrow\downarrow$	391.9	389	average; Ref. 24
Sn	$3d\downarrow$	500.7	493.6	$3d_{5/2}$; Ref. 3
	$4d\downarrow$	34.3	32.4	$4d_{5/2}$; semiempirical; Ref. 4
	$3d\downarrow \rightarrow 4d\downarrow\downarrow$	417.7		
Sb	$3d\downarrow$	544.8	536.5	$3d_{5/2}$; interpolation Cd-Xe; Ref. 4
	$4d\downarrow$	42.5		
	$3d\downarrow \rightarrow 4d\downarrow\downarrow$	444.4		
Te	$3d\downarrow$	590.5	581.9	$3d_{5/2}$; Ref. 3
	$4d\downarrow$	51.4		
	$3d\downarrow \rightarrow 4d\downarrow\downarrow$	471.3		

In order to get some idea about the splitting of the Auger energies and their free-atom–metal shifts due to the various possible initial and final states we consider the effect of the flipping a spin. This is the only way to introduce a different "term" in our spherically symmetric model. In the case of free Mg and Ag ions with two core holes the flipping of one hole spin ($\text{Mg}:2p\downarrow\downarrow \rightarrow 2p\downarrow\uparrow$, $\text{Ag}:4d\downarrow\downarrow \rightarrow 4d\downarrow\uparrow$) causes the energy to increase by 3.1 eV for Mg and 1.1 eV for Ag. These energy changes are of the same order as the differences between adjacent Auger energy lines in experimental spectra.[2,26] For core-hole ions in the jellium vacancy the energy increase in the

spin-flip process is the same in magnitude as for free ions. Thus the spectra are quite rigidly shifted when going from free atom to the atom in metal.

The important observation concerning the absolute values of the core-level binding and Auger energies is that the discrepancies (typically of the order of a few eV) with experiment, associated with approximations made (in particular, the local-density approximation and the neglect of multiplet structure), are strongly intra-atomic in nature. This means that while the approximations made do affect the position of any given spectral peak, both for the free atom and for the atom in metal, the differences between the ener-

gies corresponding to the two cases are much less sensitive to them since the intra-atomic errors largely cancel each other. The shifts, which are our principal concern, are brought about by environmental effects. We also note that while the solid environment does change the spectral characteristics, mainly via increased broadening, the shifts in, e.g., the Auger case are very similar for the various line components corresponding to the same experimental spectrum. This, of course, gives credence to our concentrating on a single "average" orbital configuration with spherical symmetry.

Table III gives the calculated shifts for the various core-level binding energies in the atom-in-jellium-vacancy model, and their experimental estimates. Recall that the common reference level is the vacuum level. There are omissions for Zn and Ag in this and the other tables because a satisfactory convergence for Zn and Ag ground-state atoms in metal was not achieved. Table IV lists the calculated free-atom-metal Auger energy shifts, again in the atom-in-jellium-vacancy model, and compares them with the experimental data due to Aksela and co-workers.[2,3] The agreement between the experimental and calculated values is gratifying, especially in the

Auger case. This is quite remarkable considering the simplicity of the model: it contains no adjustable parameters. Note also that the actual computer programs for the free atom and the atom embedded in metal are identical in the sense that the latter reduces to the former as the background density and the Fermi energy approach zero.

We have also investigated the shift in the spherical solid model proposed by Almbladh and von Barth.[12] The lattice ions surrounding the central atom were represented by local Ashcroft[27] pseudopotentials, and the summations after spherical averaging were carried out using Ewald techniques. In the case of Al (the Ashcroft core radius $r_c = 1.12$) the shift for the KLL line changed by 0.1 eV, which is negligible, especially if one keeps in mind the uncertainty associated with the experimental determination of the work function ϕ.

One noticeable feature is the near constancy of the Auger energy shifts, is especially in MNN Auger case for the six consecutive elements, Ag through Te, in the periodic table; the deviations in the shift, when both energies are referenced to the vacuum level, are less than 15%. This tendency contradicts with Shirley's "excitonic" model,[7] which predicts a rather strong increase as a function of Z.

Lang and Williams[28] have defined the Auger parameter ξ in a way which formally eliminates the reference levels

$$\xi = (B_i - B_j - B_k) - E_{ijk} \ , \tag{5}$$

where the B's are the binding energies of the core levels i, j, and k, and E_{ijk} is the Auger electron ener-

TABLE III. Core-level binding energy shifts. ΔSCF refers to the atom-in-jellium-vacancy model.

Element and hole configuration		Core-level binding energy shift Δ_{XPS}(eV)	
		ΔSCF (this work)	Experimental (Refs. 3 and 4)
Mg	$1s\downarrow$	5.1	4.9
	$2p\downarrow$	4.5	
Al	$1s\downarrow$	6.3	6.3
	$2p\downarrow$	5.8	
Cd	$3d\downarrow$	4.1	3.0
	$4d\downarrow$	3.8	
In	$3d\downarrow$	5.2	3.7
	$4d\downarrow$	4.9	
Sn	$3d\downarrow$	4.0	3.8
	$4d\downarrow$	4.0	
Sb	$3d\downarrow$	4.6	3.7
	$4d\downarrow$	4.0	
Te	$3d\downarrow$	4.6	3.6
	$4d\downarrow$	4.4	

TABLE IV. Atom-metal Auger energy shifts. ΔSCF refers to the atom-in-jellium-vacancy model. The last column gives the results of the "excited-atom" model (see text).

	Auger energy shift Δ_{Auger} (eV)		
Element	ΔSCF (this work)	Experimental (Refs. 2 and 3)	"Excited-atom" model
Mg $1s\downarrow \rightarrow 2p\downarrow\downarrow$	15.6	15.0	
Al $1s\downarrow \rightarrow 2p\downarrow\downarrow$	16.8	16.9	
Zn $2p\downarrow \rightarrow 3d\downarrow\downarrow$	14.1	13.4	
Ag $3d\downarrow \rightarrow 4d\downarrow\downarrow$	11.2	11.8	10.1
Cd $3d\downarrow \rightarrow 4d\downarrow\downarrow$	12.2	11.8	11.9
In $3d\downarrow \rightarrow 4d\downarrow\downarrow$	12.0	13.1	13.8
Sn $3d\downarrow \rightarrow 4d\downarrow\downarrow$	12.5	13.7	13.8
Sb $3d\downarrow \rightarrow 4d\downarrow\downarrow$	13.5	13.8	15.4
Te $3d\downarrow \rightarrow 4d\downarrow\downarrow$	13.9	13.3	17.7

gy for the transition, where the initial hole is in the ith level and the two final ones in the jth and kth. The calculated Auger parameters for free atoms and metals, corresponding to the transitions discussed above, are listed in Table V. We notice that the Auger parameters for the metal is about 10 eV smaller than for the free atom.

We now proceed to an interpretation and analysis of the results of our calculations. Here we have been influenced by the arguments of Lang and Williams,[14] and we generalize their ideas and extend them to the Auger case. The energy shift Δ is decomposed into the chemical shift, Δ_c, reflecting the changes in the charge state and chemical environment, and the relaxation shift Δ_r,

$$\Delta = \Delta_c + \Delta_r \ . \tag{6}$$

The two contributions cannot be measured individually, and thus the decomposition is seemingly arbitrary. For applications trying to resolve how an atom is bonded to its neighbors, it is however convenient to define Δ_c to be a property of the ground state, without any reference to the presence of core hole(s). The remaining shift is then due to the collective response of the solid to the core hole(s). Following Lang and Williams,[14] we define the chemical shift in the XPS case as

$$\Delta_c = \epsilon_i(\text{atom in metal}) - \epsilon_i(\text{free atom}) - (\epsilon_F + \phi) \ , \tag{7}$$

where i defines the state where the core hole will be created, and ϵ_i is the density-functional eigenvalue associated with the level i. In Eq. (7), both ϵ_i are understood to be measured from the "natural" reference levels, the vacuum in the atomic case and the bottom of the conduction band in the metal case. Since the bottom of the band is below the vacuum by the amount $\epsilon_F + \phi$, this has been subtracted to equal-

ize the reference levels. To a good approximation the chemical shift defined in Eq. (7) reflects only the electrostatic potential change near the nucleus. The relaxation shift Δ_r is obtained from the total shift by subtracting Δ_c as is obvious from Eq. (6). Table VI lists the chemical shifts Δ_c and the relaxation shifts Δ_r for the XPS processes considered.

The chemical shift Δ_c varies rather strongly from one element to the other. We notice that Δ_c is positive for Mg, Al, In, and Sn, nearly zero for Sb and negative for Cd and Te. A positive sign of Δ_c indicates that charge is transferred towards the nucleus in the condensed phase, which raises the energy levels. A negative Δ_c is caused by the charge transfer outwards from the nucleus. The relaxation shifts Δ_r for XPS processes are positive in all cases and they are almost independent of Z. The relaxation shift is related to the spatial distribution of the screening charge, as we shall discuss below.

In the Auger case the definition of the chemical shift [Eq. (7)] becomes slightly ambiguous, since three different orbitals and corresponding eigenvalues are involved, and the changes in ϵ_i may differ for these. If we define the chemical shift for Auger process as in Eq. (7), i standing for the state where the initial core hole will be created, the chemical shifts for the Auger transitions considered are the same as for the core levels indicated in Table VI. The Auger relaxation shifts corresponding to this definition are also given in Table VI. They are 2–3 times the relaxation shifts of the XPS lines.

However, this decomposition to chemical and relaxation shifts for the Auger process is somewhat misleading, since it is really the *difference* in the screening energy between a two-hole and one-hole configuration that is responsible for the relaxation shift. In order to emphasize this, we have also con-

TABLE V. The calculated Auger parameters [Eq. (5)].

Element		ξ_{atom} (eV)	ξ_{metal} (eV)
Mg	KLL	25.0	13.3
Al	KLL	27.2	15.7
Zn	LMM	17.4	
Ag	MNN	12.5	
Cd	MNN	13.6	4.9
In	MNN	13.6	6.3
Sn	MNN	14.4	6.0
Sb	MNN	15.5	5.4
Te	MNN	16.3	6.5

TABLE VI. The chemical shift Δ_c and the relaxation shift Δ_r for the XPS and Auger processes. The starred quantities refer to the definition [Eq. (8)] of the chemical shift for Auger emission. All energies in eV.

Element	Δ_c	Δ_r (XPS)	Δ_r (Auger)	Δ_c^*	Δ_r^*
Mg	0.4	4.7	15.2	10.3	5.4
Al	1.3	5.0	15.5	11.6	5.2
Zn				9.4	4.7
Ag				7.2	4.0
Cd	−0.8	4.9	13.1	8.0	4.2
In	0.4	4.8	11.6	8.9	4.2
Sn	0.3	3.7	12.1	9.0	3.5
Sb	0.0	4.6	13.5	8.8	4.7
Te	−0.3	4.9	14.2	8.5	5.4

sidered another definition of the chemical shift for Auger process, namely

$$\Delta_c^* = \epsilon_l^*(\text{atom in metal}) - \epsilon_l^*(\text{free atom}) - (\epsilon_F + \phi) \quad,$$

$$(8)$$

where the ϵ_l^* stand for the density-functional eigen-values for the (unfilled) initial level, calculated for systems with a core hole. This definition of the chemical shift focuses on the changes of the initial state brought about by environment, before the Auger decay but *after* the initial ionization. The values of Δ_c^* and the corresponding relaxation shift Δ_r^* for the Auger processes are also given in Table VI. Now we see that $\Delta_r^* \approx \Delta_r(\text{XPS})$ while Δ_c^* is now in every case positive and roughly twice Δ_r^*. This is na-tural since the initial core hole couples more strongly to the environment (the charge transfer towards the nucleus is larger than in the case of a neutral atom in metal; Δ_c^* "contains" the relaxation shift of a single core hole).

Lang and Williams[14] have derived an approximate formula for the relaxation shift. According to them the relaxation shift for the XPS process is half of the electrostatic potential at the nucleus due to the extra-atomic screening charge Δn

$$\Delta_r \cong \frac{1}{2} \int d\,\vec{r}\,\frac{\Delta n(\vec{r})}{r} \quad.$$

$$(9)$$

In the XPS process the extra-atomic screening charge is defined as

$$\Delta n_{\text{XPS}}(\vec{r}) = [n_{iv}(\vec{r}) - n_{ii}(\vec{r})] - [n_{iii}(\vec{r}) - n_i(\vec{r})] \quad.$$

$$(10)$$

Above n denotes charge densities and the subscripts refer to the configurations (i)−(vi) discussed in Sec. II. We have generalized the use of Eq. (9) to the Auger process by defining the corresponding extra-atomic screening charge as

$$\Delta n_{\text{Auger}}(\vec{r}) = [n_{vi}(\vec{r}) - n_{iv}(\vec{r})] - [n_v(\vec{r}) - n_{iii}(\vec{r})] \quad.$$

$$(11)$$

By charge conservation the screening-charge distribu-tions Δn_{XPS} and Δn_{Auger} contain one electron, i.e., their integral over all space is unity.

Examples of the extra-atomic screening-charge density in XPS and Auger processes are shown in Fig. 1 (see also Fig. 4 and the discussion below). For instance, in the uppermost part the full curve gives the extra-atomic screening charge in the XPS process in Mg, where there is a $1s$ core hole. The dotted line illustrates the extra-atomic screening cloud in the Auger transition in Mg, where there is a $1s$ core hole in the initial state and two $2p$ core holes in the final state. One immediate observation from the figure is the near similarity of Δn_{XPS} and Δn_{Auger}. This is not
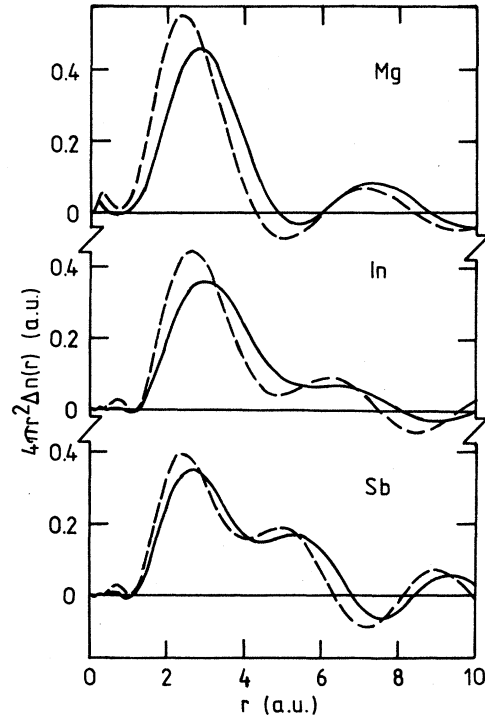

FIG. 1. Extra-atomic screening-charge densities for Mg, In, and Sb. The full and dotted curves refer to the XPS process [$\Delta n_{\text{XPS}}(r)$, Eq. (10)] and the Auger process [$\Delta n_{\text{Auger}}(r)$, Eq. (11)], respectively.

very surprising, especially if one remembers from Table VI that $\Delta_r^* \cong \Delta_r(\text{XPS})$.

We find Eq. (9) to be a reasonably good approxi-mation to the relaxation shifts. This is demonstrated in Table VII where we compare the exact calculated relaxation shifts [defined via Eq. (6) after specifying the chemical shift in Eqs. (7) or (8)] with those predicted by Eq. (9). The agreement is good espe-cially in the XPS case where the differences are of the order of estimated numerical errors. The relaxa-tion shifts for Auger processes predicted from Eq. (9) are somewhat larger than those obtained from Eq. (6). The reason for this is related to the ambiguity in the definition of the chemical shift.

The counterparts in energy space of the extra-atomic screening-charge densities are shown in Figs. 2 and 3, where we show the changes in the con-tinuum parts of the induced state densities, decom-posed into their angular momentum components. In particular, we denote

$$\Delta D(\epsilon) = \delta D^{(1)}(\epsilon) - \delta D(\epsilon) \quad,$$

$$(12)$$

$$\Delta D^*(\epsilon) = \delta D^{(2)}(\epsilon) - \delta D^{(1)}(\epsilon) \quad,$$

$$(13)$$

where δD, $\delta D^{(1)}$, and $\delta D^{(2)}$ are the induced state densities due to neutral, singly ionized and doubly

TABLE VII. The comparison of the "exact" relaxation shifts to the approximation of Eq. (9) and to the "excited-atom" model. All energies in eV.

Element	Δ_r(XPS)	Eq. (9) Δ_r(XPS)	Δ_r^*(Auger)	Eq. (9) Δ_r^*(Auger)	"Excited-atom" model Δ_r^*(Auger)
Mg	4.7	4.9	5.4	6.4	
Al	5.0	5.1	5.2	6.7	
Zn			4.7	5.9	
Ag			4.0	5.0	4.5
Cd	4.9	4.3	4.2	5.0	4.9
In	4.8	4.3	4.2	5.0	5.1
Sn	3.7	4.3	3.5	5.0	5.2
Sb	4.6	4.5	4.7	5.1	5.4
Te	4.9	4.4	5.4	5.0	5.7

ionized atoms, respectively, all embedded in a free-electron metal. Note that the integrals over the occupied region (0 to ϵ_F) over these continuum functions are variable integers, depending on whether the outermost levels are bound for the metallic atom (ion) or not (see Table VIII). For example, doubly ionized Mg in metal binds the $3s$ electrons whereas neutral Mg in metal does not. Thus $\Delta D(\epsilon)$ is the contribution of band electrons having energy ϵ to the volume integral of the extra-atomic screening charge $\Delta n_{XPS}(\vec{r})$ in Eq. (10). Likewise, $\Delta D^*(\epsilon)$ is related to $\Delta n_{Auger}(\vec{r})$ in Eq. (11). The curves plotted in Figs. 2 and 3 are not directly comparable to the local densi-

ties of states around atoms with core holes, which, with due account for selection rules and matrix elements, are reflected in the line shapes of x-ray emission and core-core-valence (CCV) Auger spectra.[29] What is shown here is the change in the (conduction) electron density between the initial and final states of the electron ejection process, decomposed in terms of
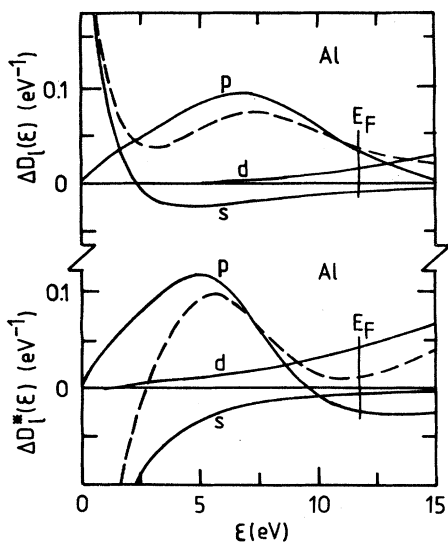

FIG. 2. Induced state densities (dotted curves) and their angular momentum components corresponding to the extra-atomic screening cloud for XPS [$\Delta D(\epsilon)$, Eq. (12)] and Auger [$\Delta D^*(\epsilon)$ Eq. (13)] processes in Al.
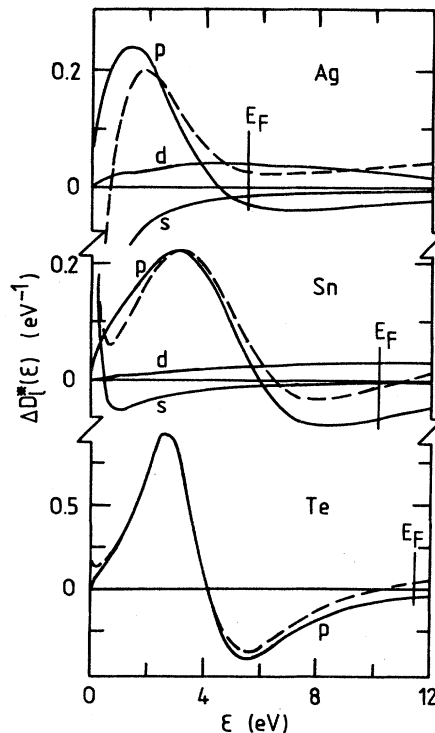
FIG. 3. Induced state densities (dotted curves) and their angular momentum components corresponding to the extra-atomic screening cloud for the Auger process in Ag, Sn, and Te [$\Delta D^*(\epsilon)$, Eq. (13)].

TABLE VIII. Bound- and continuum-electron counts for atoms in jellium vacancy with zero, one, and two core holes. Z-Z_h is the total number of induced electrons (Z is the atomic number and Z_h is the metal valency).

Element and hole configuration	Electrons in bound states		Electrons in continuum states	Z-Z_h
	↑	↓		
Mg	5	5	0	
Mg $1s\downarrow$	5	4	1	12-2
Mg $2p\downarrow\downarrow$	6	4	0	
Al	5	5	0	
Al $1s\downarrow$	5	4	1	13-3
Al $2p\downarrow\downarrow$	6	4	0	
Zn $2p\downarrow$	14	13	1	30-2
Zn $3d\downarrow\downarrow$	15	13	0	
Ag $3d\downarrow$	24	23	−1	47-1
Ag $4d\downarrow\downarrow$	24	22	0	
Cd	23	23	0	
Cd $3d\downarrow$	24	23	−1	48-2
Cd $4d\downarrow\downarrow$	24	22	0	
In	23	23	0	
In $3d\downarrow$	24	23	−1	49-3
In $4d\downarrow\downarrow$	24	22	0	
Sn	23	23	0	
Sn $3d\downarrow$	24	23	−1	50-4
Sn $4d\downarrow\downarrow$	24	22	0	
Sb	23	23	0	
Sb $3d\downarrow$	24	23	−1	51-5
Sb $4d\downarrow\downarrow$	24	22	0	
Te	24	24	−2	
Te $3d\downarrow$	24	23	−1	52-6
Te $4d\downarrow\downarrow$	24	22	0	

energy and angular momentum.

For Mg, Al, and Zn the extra-atomic screening clouds have strong s and p components. The low-energy divergence proportional to $\epsilon^{-1/2}$ in the s part of the induced state density has been discussed previously.[18,30] For the fifth-row elements, we see an increasingly strong p component for Ag through Te; the latter is completely dominated by p-wave scattering.

We now investigate the adequacy of the "excited-atom" approach[7,8] to describe the relaxation accompanying a core-hole ion in metallic environment. In the "excited-atom" approach the screened ion in metal is mimicked by transferring one core electron (or two electrons in the final state of the Auger process) to the lowest unoccupied valence orbital. Following Lang and Williams[14] we treat the excited atom fully self-consistently.

Especially, we consider extra-atomic screening

cloud in the Auger process and the Auger energy shifts for elements Ag through Te. The situation is similar for the XPS process as can be expected from extra-atomic screening-charge densities of Fig. 1 and we do not consider the XPS process here. Figure 4 shows the extra-atomic screening-charge density in the Auger process for Ag, Sn, and Te. The full and dotted curves give the screening charge calculated using the atom-in-jellium-vacancy and the "excited-atom" models, respectively. The former is defined by Eq. (11) and the latter is

$$\Delta n^{*}_{\text{Auger}}(\vec{r}) = [n^{*}_{\text{vi}}(\vec{r}) - n^{*}_{\text{iv}}(\vec{r})] - [n_{\text{v}}(\vec{r}) - n_{\text{iii}}(\vec{r})]$$

(14)

where n^{*}_{vi} and n^{*}_{iv} are the charge densities of neutral
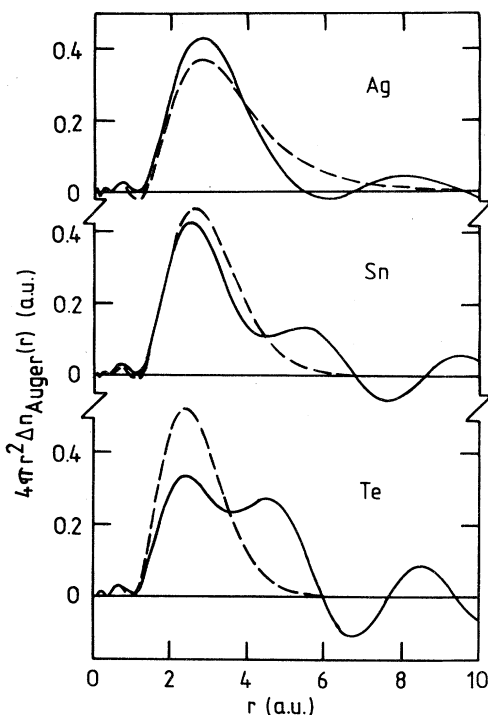
FIG. 4. Extra-atomic screening-charge densities for Ag, Sn, and Te in the Auger process. The full curve is obtained using the atom-in-jellium-vacancy model [$\Delta n_{Auger}(r)$, Eq. (11)]. The dotted curve is obtained using the "excited-atom" model [$\Delta^* n_{Auger}$, Eq. (14)].

excited free atoms with one and two core holes, respectively. We see that in the case of Ag and Sn the "excited-atom" model reproduces rather well the overall distribution of the extra-atomic screening cloud, especially the hump between $r \cong 1.5$ a.u. and $r \cong 4$ a.u. Of course the "excited-atom" model does not reproduce the Friedel oscillations obtained in atom-in-jellium-vacancy model and when the nuclear charge Z increases it looks like a second hump is growing up from the first maximum of oscillations. For Te the two humps are nearly equal in height and the "excited-atom" model is expected to be inadequate. The formation of a second hump is also seen in extra-atomic screening clouds of atoms chemisorbed on metal surfaces.[14] Quantitatively the accuracy of the "excited-atom" model is seen by comparing the values of the relaxation shifts obtained from Eq. (9) in Table VII. The "excited-atom" model reproduces quite accurately the Δ_r^* (Auger) values for Cd, In, and Sn. However, the "excited-atom" model gives an increasing trend and for Sb and especially for Te Δ_r^* (Auger) obtained in the "excited-atom" model is considerably greater than Δ_r^* (Auger) obtained in atom-in-jellium-vacancy model.

The above discussion confirms the notion[28] that in the "excited-atom" model the screening of the ion

by the free valence electrons is inadequately mimicked when the valence electrons cannot penetrate inside the bound shells. In the present case this means that in the screening of the ion the role of the second hump, Fig. 4, which is formed by unbound valence electrons, becomes important as Z increases. From the energy-space decompositions in Fig. (3) we can conclude that the second hump is due to the p-like resonance which appears and grows up in the density of states when moving from Ag towards Te.

In Table IV we list also the values for the Auger shifts for Ag through Te obtained using the "excited-atom" model. These values depend remarkably on the nuclear charge Z; the Auger shift increases from 10.1 to 17.7 eV. This strong dependence on Z is evident also in other calculations for elements Ag through Te which are based on similar "excited-atom" models.[26]

IV. CONCLUSIONS

The calculations based on ΔSCF density-functional methods reproduce well the Auger and core-level binding energy shifts for a number of metallic elements. The chemical shifts of neutral ground-state atoms embedded in metal depend on the details of the system under investigation, but are generally small. The corresponding relaxation shifts are large, but rather insensitive to the system at hand. The atom-in-jellium-vacancy model gives a good description as far as the deep core-level shifts are considered, which corroborates the role of the metal simply being a rather structureless reservoir of screening electrons. The relaxation shift Δ_r in the Auger process (when the chemical shift is defined for the neutral ground-state atom) is up to three times that for the XPS process, which indicates substantial nonlinearities in the response.

The "excited-atom" model has also been tested. When treated fully self-consistently, it gives a qualitatively correct description of the extra-atomic response and shifts when the unoccupied valence shell can accommodate the screening charge. However, it fails drastically when this is not the case, and, for example, predicts an incorrect increasing trend in the Auger shift in going from Ag to Te.

Extension of the present approach to dilute alloys (e.g., $3d$ impurities in aluminium[31]) and impurity systems (e.g., rare-gas implants in metals,[32] and the so-called charge-transfer insulators[33]) would seem worth considering.

ACKNOWLEDGMENTS

[1]See, for example, *Topics in Applied Physics,* edited by M. Cardona and L. Ley (Springer, Berlin, 1978), Vols. 26 and 27.

[2]S. Aksela, R. Kumpula, H. Aksela, J. Väyrynen, R. M. Nieminen, and M. Puska, Phys. Rev. B 23, 4362 (1981).

[3]S. Aksela, R. Kumpula, H. Aksela, and J. Väyrynen (unpublished).

[4]B. Johansson and N. Mårtensson, Phys. Rev. B 21, 4427 (1980).

[5]P. Steiner, S. Hüfner, N. Mårtensson, and B. Johansson, Solid State Commun. 37, 73 (1981).

[6]A. R. Miedema, R. Boom, and F. R. de Boer, J. Less Common Met. 41, 283 (1975).

[7]D. A. Shirley, Phys. Rev. A 7, 1520 (1973); L. Ley, S. P. Kowalczyk, F. R. McFeely, R. A. Pollak, and D. A. Shirley, Phys. Rev. B 8, 2392 (1973).

[8]R. E. Watson, M. L. Perlman, and J. F. Herbst, Phys. Rev. B 13, 2358 (1976); R. E. Watson, J. F. Herbst, and J. W. Wilkins, *ibid.* 14, 18 (1976).

[9]A. R. Williams and N. D. Lang, Phys. Rev. Lett. 40, 954 (1978).

[10]P. S. Bagus, Phys. Rev. 139, A619 (1965).

[11]W. Kohn and L. J. Sham, Phys. Rev. 140, A1133 (1965); U. von Barth and L. Hedin, J. Phys. C 5, 1629 (1972).

[12]C. O. Almbladh and U. von Barth, Phys. Rev. B 13, 3307 (1976).

[13]G. W. Bryant and G. D. Mahan, Phys. Rev. B 17, 1744 (1978).

[14]N. D. Lang and A. R. Williams, Phys. Rev. B 16, 2408 (1977).

[15]O. Gunnarsson and B. I. Lundqvist, Phys. Rev. B 13, 4274 (1976).

[16]See, e.g., O. Gunnarsson, in *Electrons in Disordered Metals and at Metallic Surfaces,* edited by P. Phariseau, B. L. Györffy, and L. Scheire (Plenum, New York, 1979), p. 1.

[17]M. Manninen, P. Hautojärvi, and R. Nieminen, Solid State Commun. 23, 795 (1977).

[18]M. J. Puska, R. M. Nieminen, and M. Manninen, Phys. Rev. B 24, 3037 (1981).

[19]The values used were from the tabulation by J. Hölzl and F. K. Schulte, in *Springer Tracts in Modern Physics* (Springer, Heidelberg, 1979), Vol. 85.

[20]W. Mehlhorn, B. Breuckmann, and D. Hausamann, Phys. Scr. 16, 177 (1977).

[21]J. Väyrynen, S. Aksela, and H. Aksela, Phys. Scr. 16, 452 (1977).

[22]J. Väyrynen, S. Aksela, M. Kellokumpu, and H. Aksela, Phys. Rev. A 22, 1610 (1980).

[23]Unpublished results by S. Aksela *et al.*

[24]S. Aksela, J. Väyrynen, H. Aksela, and S. Pennanen, J. Phys. B 13, 3745 (1980).

[25]K. N. Huang, M. Ayoagi, M. Chen, B. Crasemann, and H. Mark, At. Data Nucl. Data Tables 18, 243 (1976).

[26]M. Pessa, A. Vuoristo, M. Vulli, S. Aksela, J. Väyrynen, T. Rantala, and H. Aksela, Phys. Rev. B 20, 3115 (1979).

[27]N. W. Ashcroft and D. C. Langreth, Phys. Rev. 155, 682 (1967).

[28]N. D. Lang and A. R. Williams, Phys. Rev. B 20, 1369 (1979).

[29]R. Lässer and J. C. Fuggle, Phys. Rev. B 22, 2637 (1980).

[30]J. E. Inglesfield and J. B. Pendry, Philos. Mag. 34, 205 (1976); J. K. Nørskov, Phys. Rev. B 20, 446 (1979).

[31]P. Steiner, H. Höchst, W. Steffen, and S. Hüfner, Z. Phys. B 38, 1919 (1980); R. M. Nieminen and M. Puska, J. Phys. F 10, L 123 (1980).

[32]P. H. Citrin and D. R. Hamann, Phys. Rev. B 10, 4948 (1974).

[33]R. Avci and C. P. Flynn, Phys. Rev. B 19, 5967 (1979); R. M. Nieminen and M. Puska, Solid State Commun. 33, 463 (1980).